International Journal of Mass Spectrometry 450 (2020) 116306

Contents lists available at ScienceDirect

International Journal of Mass Spectrometry

journal homepage: www.elsevier.com/locate/ijms

Strategies for avoiding saturation effects in ESI-MS

Alan An Jung Wei , Anuj Joshi , Yuxuan Chen , J. Scott McIndoe *

Department of Chemistry, University of Victoria, PO Box 1700 STN CSC, Victoria, BC, V8W 2Y2, Canada

ARTICLE INFO

Article history:
Received 30 September 2019
Received in revised form
9 January 2020
Accepted 28 January 2020
Available online 30 January 2020

ABSTRACT

All instruments with detectors are prone to saturation effects at high concentration, and mass spectrometers are no exception. The very high sensitivity of mass spectrometry makes the onset of saturation occur at lower concentrations than other methods, and in cases where the analyte of interest is very reactive, concentrations at which saturation can be problematic may be necessary in order to ensure decomposition is mitigated. Indications that saturation is occurring are provided, and some data processing strategies are outlined, followed by a range of detuning strategies that can be employed to reduce saturation effects in the context of electrospray ionization mass spectrometry (ESI-MS), including lowering voltages on detector or capillary, increasing cone gas flow rates, or adjusting the probe position. A combination of strategies generally allows researchers to make the best possible compromises when studying reactive compounds at relatively high concentration.

1. Introduction

Mass spectrometrists are tireless in their search for sensitivity [1]. Instrumentation and methodologies are in constant development in order to push the limits of detection lower and the linear dynamic range wider, and astonishing feats of characterization have been achieved as a result. For most chemists, and particularly those hunting trace analytes or dealing with incredibly complicated mixtures of biological origin, this quest is an entirely desirable one. However, some scientists use mass spectrometry to monitor the reactions of highly reactive compounds [2–4], and the raw sensitivity of the technique can prove to be a double-edged sword. Highly reactive compounds will interact rapidly and deleteriously with both oxygen and moisture [5–7], which are difficult to remove from solvents beyond 5 ppm. Yet mass spectrometers can effortlessly characterize charged species at this level, and far below. So we have a conundrum: on one hand, we want to run the analysis at as high a concentration as possible, because dilution will not only greatly slow the rate at which the reaction we are interested in will occur, it will also introduce relatively large quantities of undesirable compounds that can cause analyte decomposition. On the other hand, high concentrations are problematic for mass spectrometric analysis [8], causing issues of ion suppression [9], space-charge effects that affect transmission efficiency [10], and saturation.

The main obstacle caused by saturation is the inability to acquire an accurate quantification of species [11], as the spectrum no longer reflects the "real" concentration of the sample. There are a few possibilities that explain the phenomenon of saturation due to a higher concentration. Aside from the previously mentioned ion suppression, the finite amount of excess charge [12] and the limited space [13] on droplet surfaces could give rise to saturation. Imaginative use of algorithmic correction has been reported [14], whereby an unsaturated peak in an isotope pattern is used to work backwards to a more accurate estimation of the abundance of that species. In cases where we are operating at concentrations at which saturation effects become troublesome, we deliberately detune the mass spectrometer. By adjusting various instrumental parameters, the analyte response can be improved and optimized [15]. The effect on the ion intensity can be greatly affected by the solvent of choice, the gas flow rate [16], and the source temperature settings of the instrument [17]. This work describes the indications of saturation and some of the parameters we change in order to obviate the effects of this phenomenon.

In this study, we primarily examined the trityl carbocation, $[Ph_3C]^+$, a reactive ionic compound used to abstract hydride or methide [18]. It is stable in the presence of a weakly coordinating anion (in this case, $[B(C_6F_5)_4]^-$), and as it is permanently positively charged, it is easy to detect using electrospray ionization mass spectrometry (ESI-MS). A common issue that is encountered for mass spectrometric analyses of highly reactive chemicals is sample decomposition at lower concentrations. As for trityl carbocation,

* Corresponding author.
E-mail address: mcindoe@uvic.ca (J.S. McIndoe).

https://doi.org/10.1016/j.ijms.2020.116306
1387-3806/

data acquisition becomes challenging when the sample is at micromolar concentrations. An alternative solution is necessary when diluting the concentration has simply impractical. Our study details ways to detune the instrumental settings with a quadrupole time-of-flight (QTOF) mass spectrometer that contains a time-to-digital converter (TDC) microchannel plate detector (MCP).

2. Results and discussion

2.1. Evidence for saturation

Saturation can be indicated by various observations from a mass spectrum. The observations below are a guide of identifying saturation recorded on a mass spectrum. A combination of more than one scenario listed below serves as good indications of necessary instrumental detuning to avoid saturation that cannot be trouble-shot by simply dialing down the sample concentration.

2.1.1. Peak shape

To identify saturation from a mass spectrum, peak shape is distorted mostly at the base of the peak. In a time-of-flight mass analyzer (TOF), a peak shape that indicates saturation is illustrated in Fig. 1. By zooming in on a full-scale spectrum (1a) and examining the baseline (1b), a distinct ramp is evident before the peak.

Saturation can also be identified by the distortion at the top of the peak. It gets truncated so that the peak shape is squared off. In a mass spectrometer with a triple quadruople mass analyzer (TQD), tuning the resolution shows a significant effect on the quality of spectrum as the higher the resolution can be indicated by a sharper peak (Fig. 2). By increasing the resolution of the mass analyzers, saturation effects are mitigated.

2.1.2. Isotope pattern shape

Saturation disproportionately affects the most intense peaks on the spectrum. Due to the fact that isotope patterns contain peaks of different intensity, they are affected to different degrees. In practice, this means that the smaller peaks are larger than they should be, and the more intense peaks are less intense than anticipated. For hydrocarbon species, the ratio between the isotope pattern of M, the mass of the most abundant isotope, and M+1, should be 5:1 (Fig. 3(b) [19]). In this example, trityl cation, $[Ph_3C]^+$, has a less abundant peak at *m/z* 243 and a more abundant isotope peak at *m/z* 244 (Fig. 3(a)). The order of intensities, however, does not change.

The fact that the less abundant peaks are not saturated is a fact

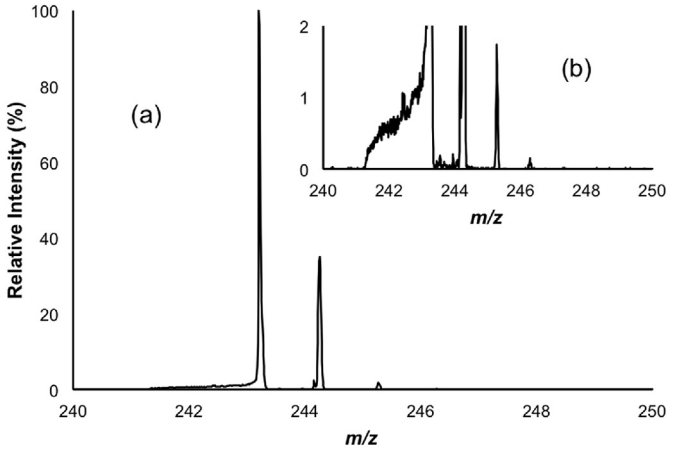

Fig. 1. Peak shape of a saturated peak (a) full scale and (b) zoomed into the y axis by a factor of 20 indicated by a time-of-flight mass analyzer (TOF).

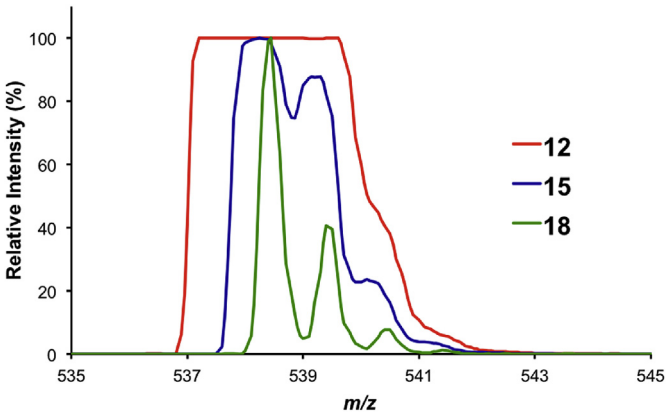

Fig. 2. Peak shape of a saturated peak (red, resolution at 12), and nonsaturated (blue, resolution at 15 and green, resolution at 18) from a triple quadrupole mass analyzer (TQD). (For interpretation of the references to colour in this figure legend, the reader is referred to the Web version of this article.)

that can be exploited when tracking reactions as indicated and explained in detail in the next section.

2.1.3. Reaction traces

One negative effect of saturation is the inaccuracy of reaction traces. Plotting reaction progress with a saturated peak gives data that is not only unreliable but non-physical. It is most often characterized by a reactant that barely seems to diminish while a product appears to a large extent. As the reaction proceeds, the product itself may become saturated and the trace climbs less than it should while the trace of reactant diminishes normally. These behaviours can be observed in Fig. 4(a). The red line drops in intensity by approximately 1600 counts during which period (about the first 30 s of reaction) the blue line rises to ~3200 counts. In this particular example, two reactions are occurring, neutralization and isobutylation of trityl, and only the isobutylation product is observed as indicated by the decline of both traces.

A useful and quick test for saturation involves looking at the traces for individual peaks in the isotopomer envelope. If none of the peaks is saturated, all of the traces should overlay once normalized (though the lower abundance peaks will necessarily generate a noisier trace). If the abundant peaks show divergent behaviour, saturation effects are likely in play. Fig. 4(b) (for M+1) shows quite different behaviour to Fig. 4(a), and is a much better representation of the actual solution behaviour. Fig. 4(c) is for the M+2 peak, which is low enough in intensity enough that the trace becomes rather noisy, but the trace is closer in behavior to 4(b) than to 4(a).

Understanding saturation effects is crucial to correct interpretation of the abundance traces in a reaction [20,21]. Sample dilution might be the first troubleshooting that comes to mind, however, a simple dilution is not ideal as it can often complicates the problem [22]. As reaction rate is closely associated with the sample concentration, a more dilute sample can slow down the reaction considerably, to the point that monitoring the reaction becomes an inefficient use of instrument time. Moreover, when handling extremely moisture- and air-sensitive compounds, even the slightest traces can decompose the samples making the reaction monitoring impossible [23].

Experimental and data processing steps can overcome the problem of saturation where dilution is not a practical solution due to analyte reactivity, as outlined below.

2.2. Mitigating saturation

Various experimental strategies can be employed if saturation is

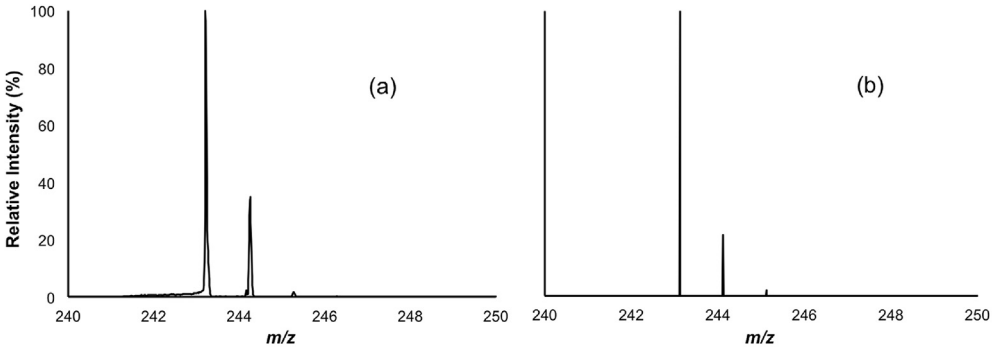

Fig. 3. Isotope pattern shape of (a) saturated spectrum and (b) calculated spectrum of trityl cation $[Ph_3C]^+$.

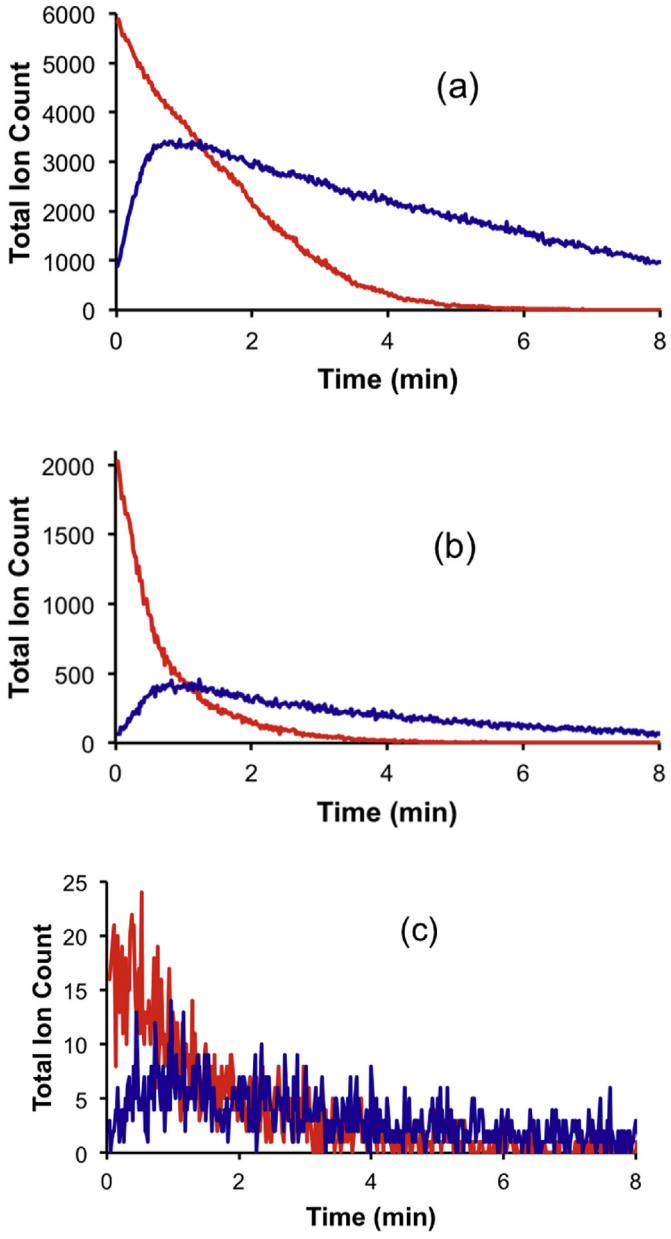

Fig. 4. Reaction between $[Ph_3C]^+$ and triisobutylaluminum (red) trityl peak $[Ph_3C]^+$ and (blue) isobutylated trityl peak $[Ph_2C_6H_4iBu]^+$. (a) M (*m/z* 243 and 299) (b) M+1 (*m/z* 244 and 300) (c) M+2 (*m/z* 245 and 301). (For interpretation of the references to colour in this figure legend, the reader is referred to the Web version of this article.)

a problem at high concentrations. Not all will be available on all instruments, and instruments other than the ones we have may very well have other options available. Here we report the instrumental parameters most effective for reducing saturation in a quadrupole time-of-flight (Q-TOF) mass spectrometer.

All samples were prepared and diluted with fluorobenzene as the solvent. The flow rate was set at 20 μL/min with a syringe pump. Five parameters of the mass spectrometer: the cone size, the microchannel plate detector voltage, the capillary voltage, the probe position, and the cone gas flow were examined. Four parameters were held constant while examining one particular parameter to allow comparisons. The optimal setting of each parameter is indicated by a linear calibration curve that corresponds to the increase of sample concentration. Curvature of the calibration response indicates saturation and more de-tuning has to be done.

2.2.1. Probe position (capillary to cone distance)

Some instruments allow the position of the capillary to be moved with respect to the orifice leading into the mass spectrometer. Moving this position can cause quite dramatic changes in signal intensity as the electric field strength is altered upon a change of capillary to cone distance [24], and the relative abundance of ions can even change [25] (with smaller, more mobile ions losing less intensity with respect to their bulkier counterparts at greater distances). Five different capillary to cone distances were chosen and investigated (positions labelled in Fig. 5) and the results were compared (Fig. 6).

The optimal probe position that indicates linear ion response according to the concentration of the analyte is the probe position 2. This probe position was therefore held constant for the acquisition of the other experimental results in this paper. Position 4 provided no response at all, position 1 (and to a lesser extent 3) were saturation-prone and position 5 provided only a weak signal and then only at moderate concentrations.

2.2.2. Detector sensitivity

Saturation affects the detector in mass spectrometers: essentially, it reaches a point at which ions are arriving at the detector but are not registered. In orthogonal time-of-flight instruments, which use microchannel plate (MCP) detectors, saturation is straightforward to understand, because MCPs can only register one event in a given time window. The data acquisition is recorded by a time to digital converter (TDC). Therefore, if at any given interval more than one ion arrival occurs, only one arrival is registered. This phenomenon is known as “digital dead time”. Because the sensitivity of the MCP is dependent on the voltage applied to it [26], in order to specifically address this issue that comes from a TDC system, an obvious approach to reducing sensitivity is to lower that

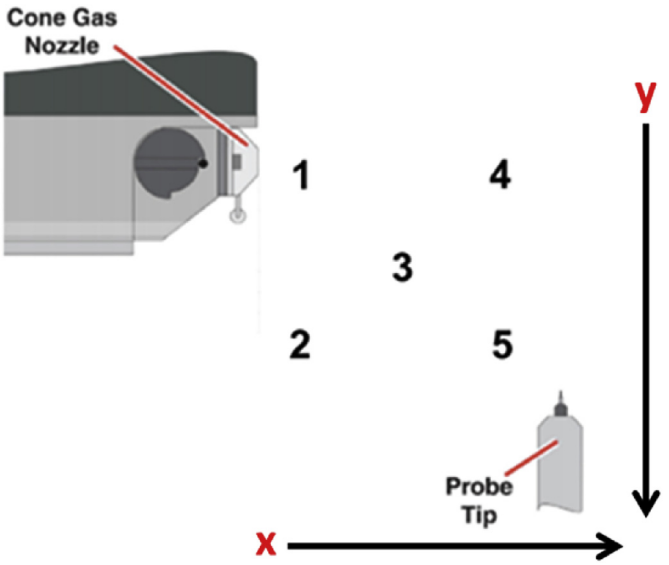

Fig. 5. Probe positions (capillary tip to cone distance) investigated. Position 1 (x = 1 mm, y = 3 mm). Position 2 (x = 1 mm, y = 6 mm). Position 3 (x = 5 mm, y = 4.5 mm). Position 4 (x = 10 mm, y = 3 mm). Position 5 (x = 10 mm, y = 6 mm).

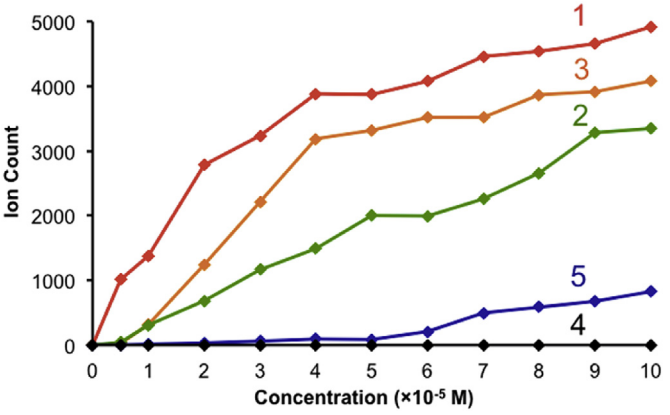

Fig. 6. Calibration curves where the cone size (0.36 mm), the cone gas flow (50L/hour), the MCP detector voltage (2500 V), and the capillary voltage (2700 V) were all held constant and only the probe position changed. Numbers indicate the probe position accordingly (Position 1 in red, position 3 in orange, position 2 in green, position 5 in blue, and position 4 in black). (For interpretation of the references to colour in this figure legend, the reader is referred to the Web version of this article.)

voltage. However, this approach has its own issues, particularly with thresholding, as seen in Fig. 7. At 2700 V, saturation is clearly a problem, with curvature of the line being apparent very early in the trace. 2500 V is close to linear, but the lower voltage values do not start registering ions at all.

2.2.3. Capillary voltage

Ionization source parameters are optimized to achieve better sensitivity of the instrument [27]. One of the main parameters of the ionization source, namely the capillary voltage applied to the spray capillary, serves multiple functions. It enables the electrospray plume to form [28] and powers the underlying electrochemistry that generates the excess of positive ions needed for analysis [29]. Ion counts usually increase with capillary voltage, but there is a limited range available. The quality of the electrospray is highly dependent on the capillary voltage, as the formation of charged droplets is closely associated with a high voltage of the

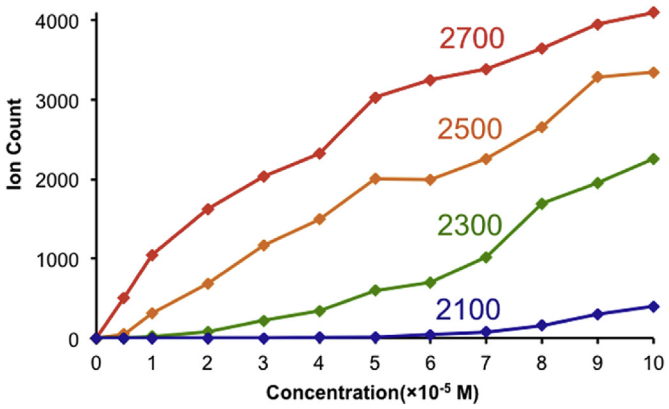

Fig. 7. Calibration curves where the cone size (0.36 mm), the probe position (position 2), the cone gas flow (50 L/h), and the capillary voltage (2750 V) were all held constant and only the MCP detector voltage changed (2700V in red, 2500V in orange, 2300V in green, and 2100V in blue). (For interpretation of the references to colour in this figure legend, the reader is referred to the Web version of this article.)

capillary [30]. Below a certain value, the electrospray plume will not form properly, and above a certain value, plasma discharges can form. Both of these manifest as highly erratic signals. Increasing the capillary voltage from 2000 V to 3000 V in increments of 250 V show that moderate values gives the most linear response (Fig. 8); high values are prone to saturation and lower values show signs of thresholding effects, requiring a certain minimal concentration before any response at all is registered. The optimum capillary voltage was at 2750 V for this particular analyte in terms of achieving reasonably linearity.

2.2.4. Cone gas flow

There are two sources of source gases on the instrument, the desolvation gas, a coaxial flow emerging from around the capillary, and the cone gas, a flow emerging from the cone mounted at the orifice of the instrument. Increasing the cone gas has the effect of increasing desolvation but at highest values it can also make it harder for the ions to make their way from source to instrument [31] and can reduce the efficiency of ionization [32,33]. Adjusting the cone gas has similar effect to the MCP voltage, despite a dramatically different mechanism of action (Fig. 9).

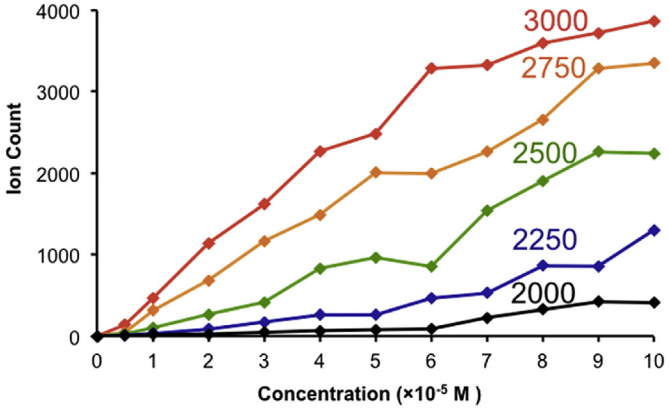

Fig. 8. Calibration curves where the cone size (0.36 mm), the probe position (position 2), the MCP detector voltage (2500 V), and the cone gas flow (50 L/h) were all held constant and only the capillary voltage changed (3000 V in red, 2750 V in orange, 2500 V in green, 2250 V in blue, and 2000 V in black). (For interpretation of the references to colour in this figure legend, the reader is referred to the Web version of this article.)

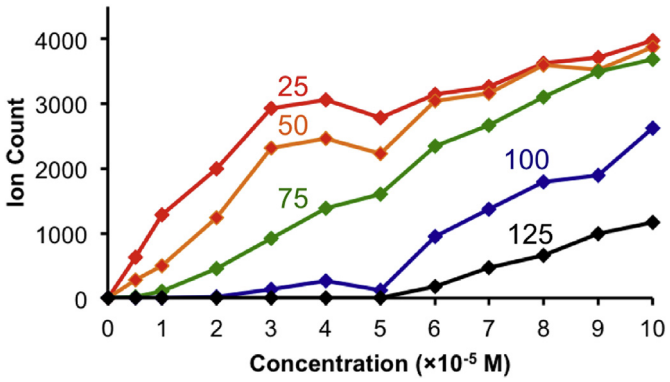

Fig. 9. Calibration curves where the cone size (0.36 mm), the probe position (position 2), the MCP detector voltage (2500 V), and the capillary voltage (2750 V) were all held constant and only cone gas flow (L/hour) changed (25 L/h in red, 50 L/h in orange, 75 L/h in green, 100 L/h in blue, and 125 L/h in black). (For interpretation of the references to colour in this figure legend, the reader is referred to the Web version of this article.)

The results agreed with our hypothesis. Lowering the cone gas flow indeed shows a better desolvation, giving a much higher ion count but with the cost of saturation. With increments of 25 L/h, we have found that in order to acquire the best linear curve, it is best to hold the cone gas flow at 75 L/h for the solvent and concentration range considered here. This value is likely to be different for other solvents.

2.2.5. Cone size

The ion count as seen on the spectrum correlates to the number of ions entering from the sampling cone of the mass spectrometer. Tuning the amount of incoming ions is an effective way to avoid saturation as it affects the ion transmission efficiency [34] and detunes the sensitivity of the instrument. Two cones, with diameters of 0.80 mm, the cone that is more commonly used for mass spectrometric experiments, and 0.36 mm, the less commonly used, were experimented with and the effect of the cone size was investigated (Fig. 10).

Comparing the two cone sizes, our experimental results have shown the dramatic effect caused by the large difference in the number of ions entering the mass spectrometer. A smaller cone size that effectively avoids the saturation issue is used for acquiring experimental results.

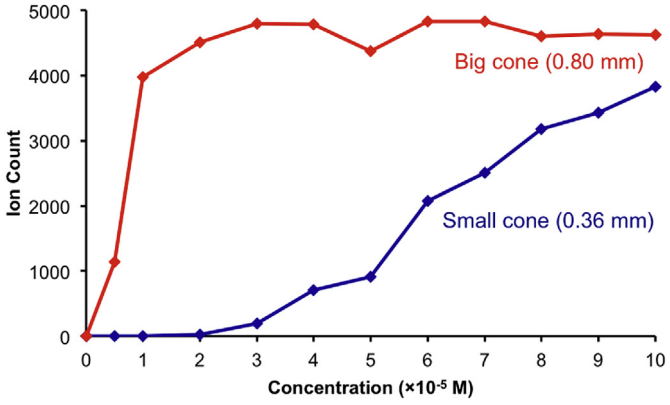

Fig. 10. Calibration curves where the probe position (position 2), the MCP detector voltage (2500 V), the capillary voltage (2700 V), and the cone gas flow (50 L/h) all held constant and only the cone size changed.

Besides de-tuning settings of a mass spectrometer to combat the saturation issue, recent instrumental developments have taken into the consideration of the saturation issue of mass spectrometer, as some modern instruments also sometimes possess settings that allow attenuation of the ion beam after the source but before encountering the mass analyzer(s). The Synapt G2Si, for example, has a setting called Continuum Dynamic Range Enhancement (DRE) [35] that introduces a baffle that diminishes the ion current making it into the mass spectrometer proper.

3. Experimental

Experiments were performed with a Waters Micromass Q-ToF Micro Mass Spectrometer. Trityl tetrakis(pentafluorophenyl)borate, $[Ph_3C]^+[B(C_6F_5)_4]^-$, (1.0 mg, 1.0×10^{-4} mol) was weighed out and fluorobenzene (10 mL) was added to prepare a solution with a concentration of 100 μM (1.0×10^{-4} M). Fluorobenzene was dried with calcium hydride (CaH_2) overnight and distilled, kept over 4 Å activated molecular sieves prior to use to get rid of traces of moisture and sample was prepared in a glovebox under nitrogen atmosphere to avoid exposure to oxygen. Calibration curves were generated via the external calibration method.

Twelve sample concentrations from 5 to 100 μM (5.0×10^{-6} to 1×10^{-4}) were prepared upon further dilution. Through a PTFE tubing that is connected directly from the glovebox into the mass spectrometer, sample was then injected via direct sample infusion from the inside of the glovebox with a 1 mL syringe and a syringe pump set at a flow rate of 20 μL/min. For each parameter adjusted, a different ESI-MS(+) spectrum was acquired for 1 min where an average the total ion count at the ion peak *m/z* 243 Da was taken. A plot of ion intensity vs. concentration was generated.

4. Conclusions

When a sample requires a higher concentration (>10 μM) due to the high reactivity of an analyte (e.g. one that reacts with trace amounts of oxygen and water), there are a range of strategies that can be employed to mitigate the inevitable saturation effects in mass spectrometric experiments. An optimal combination of the capillary voltage, the cone gas flow, the detector voltage, capillary to cone distance, and the cone size, calibration curves that better reflect ion concentration can be generated. These experimental detuning processes deliberately lower instrumental sensitivity, and can be used in tandem with data processing that focuses on examining only those isotopomers for which saturation is not problematic. Researchers have a variety of approaches when facing the difficult trade-off between minimizing decomposition of their reactive sample vs. high concentrations causing saturation effects, with the caveat that the optimum values described here are likely to be different in other instruments/solvents/analytes of interest.

Declaration of competing interest

The authors declare that they have no known competing financial interests or personal relationships that could have appeared to influence the work reported in this paper.

CRediT authorship contribution statement

Alan An Jung Wei: Investigation, Writing - original draft, Visualization, Methodology. **Anuj Joshi:** Methodology, Writing - review & editing. **Yuxuan Chen:** Investigation, Validation. **J. Scott McIndoe:** Conceptualization, Resources, Writing - review & editing, Supervision, Visualization, Funding acquisition.

Acknowledgements

J. S. M. thanks NSERC and NOVA Chemicals' Centre for Applied Research (Strategic Project Grant # 478998-15) for operational funding and CFI, BCKDF, and the University of Victoria for infrastructural support.

Appendix A. Supplementary data

Supplementary data to this article can be found online at https://doi.org/10.1016/j.ijms.2020.116306.

References

[1] J.B. Fenn, M. Mann, C.K. Meng, S.F. Wong, C.M. Whitehouse, Electrospray ionization for mass spectrometry of large biomolecules, Science 80 (1989), https://doi.org/10.1126/science.2675315.
[2] H.S. Zijlstra, A. Joshi, M. Linnolahti, S. Collins, J.S. McIndoe, Modifying methylalumoxane via alkyl exchange, Dalton Trans. (2018), https://doi.org/10.1039/C8DT04242J.
[3] L.P.E. Yunker, Z. Ahmadi, J.R. Logan, W. Wu, T. Li, A. Martindale, A.G. Oliver, J.S. McIndoe, Real-time mass spectrometric investigations into the mechanism of the Suzuki-Miyaura reaction, Organometallics (2018), https://doi.org/10.1021/acs.organomet.8b00705.
[4] R. Theron, Y. Wu, L.P.E. Yunker, A.V. Hesketh, I. Pernik, A.S. Weller, J.S. McIndoe, Simultaneous orthogonal methods for the real-time analysis of catalytic reactions, ACS Catal. (2016), https://doi.org/10.1021/acscatal.6b01489.
[5] H.S. Zijlstra, S. Collins, J.S. McIndoe, Oxidation of methylalumoxane oligomers, Chem. Eur J. (2018), https://doi.org/10.1002/chem.201705458.
[6] D. Yeung, J. Penafiel, H.S. Zijlstra, J.S. McIndoe, Oxidation of titanocene(III): the deceptive simplicity of a color change, Inorg. Chem. (2018), https://doi.org/10.1021/acs.inorgchem.7b02705.
[7] H.S. Zijlstra, M. Linnolahti, S. Collins, J.S. McIndoe, Additive and aging effects on methylalumoxane oligomers, Organometallics (2017), https://doi.org/10.1021/acs.organomet.7b00153.
[8] C.M. Alfaro, A.O. Uwakweh, D.A. Todd, B.M. Ehrmann, N.B. Cech, Investigations of analyte-specific response saturation and dynamic range limitations in atmospheric pressure ionization mass spectrometry, Anal. Chem. (2014), https://doi.org/10.1021/ac502984a.
[9] P. Kebarle, L. Tang, From ions in solution to ions in the gas phase - the mechanism of electrospray mass spectrometry, Anal. Chem. (1993), https://doi.org/10.1021/ac00070a001.
[10] J.S. Page, R.T. Kelly, K. Tang, R.D. Smith, Ionization and transmission efficiency in an electrospray ionization-mass spectrometry interface. https://doi.org/10.1016/j.jasms.2007.05.018, 2007.
[11] D.G. Beach, W. Gabryelski, Linear and nonlinear regimes of electrospray signal response in analysis of urine by electrospray ionization-high field asymmetric waveform ion mobility spectrometry-MS and implications for nontarget quantification, Anal. Chem. (2013), https://doi.org/10.1021/ac3027542.
[12] C.G. Enke, A predictive model for matrix and analyte effects in electrospray ionization of singly-charged ionic analytes, Anal. Chem. (1997), https://doi.org/10.1021/ac970095w.
[13] D.R. Zook, A.P. Bruins, On cluster ions, ion transmission, and linear dynamic range limitations in electrospray (ionspray) mass spectrometry, Int. J. Mass Spectrom. Ion Process. (2002), https://doi.org/10.1016/s0168-1176(96)04511-9.
[14] A. Bilbao, B.C. Gibbons, G.W. Slysz, K.L. Crowell, M.E. Monroe, Y.M. Ibrahim, R.D. Smith, S.H. Payne, E.S. Baker, An algorithm to correct saturated mass spectrometry ion abundances for enhanced quantitation and mass accuracy in omic studies, Int. J. Mass Spectrom. (2018), https://doi.org/10.1016/j.ijms.2017.11.003.
[15] M.A. Raji, K.A. Schug, Chemometric study of the influence of instrumental parameters on ESI-MS analyte response using full factorial design, Int. J. Mass Spectrom. (2009), https://doi.org/10.1016/j.ijms.2008.10.013.
[16] S. Gangula, M. Nimtz, P. Mischnick, Relative ion intensities of maltooligosaccharide ethers in electrospray ionization ion trap mass spectrometry: a quantitative evaluation, Int. J. Mass Spectrom. 402 (2016) 57–65, https://doi.org/10.1016/j.ijms.2016.01.009.
[17] E. Janusson, A.V. Hesketh, K.L. Bamford, K. Hatlelid, R. Higgins, J.S. McIndoe, Spatial effects on electrospray ionization response, Int. J. Mass Spectrom. (2015), https://doi.org/10.1016/j.ijms.2015.07.016.
[18] S.R. Bahr, P. Boudjouk, Trityl tetrakis[3,5-bis(trifluoromethyl)phenyl]borate: a new hydride abstraction reagent, J. Org. Chem. (2005), https://doi.org/10.1021/jo00046a048.
[19] L. Patiny, A. Borel, ChemCalc: a building block for tomorrow's chemical infrastructure, J. Chem. Inf. Model. (2013), https://doi.org/10.1021/ci300563h.
[20] R.G. Belli, Y. Wu, H. Ji, A. Joshi, L.P.E. Yunker, J.S. McIndoe, L. Rosenberg, Competitive ligand exchange and dissociation in Ru indenyl complexes, Inorg. Chem. (2019), https://doi.org/10.1021/acs.inorgchem.8b02915.
[21] E. Janusson, H.S. Zijlstra, P.P.T. Nguyen, L. Macgillivray, J. Martelino, J.S. McIndoe, Real-time analysis of Pd2(dba)3 activation by phosphine ligands, Chem. Commun. (2017), https://doi.org/10.1039/c6cc08824d.
[22] Y. Wu, L. Li, Sample normalization methods in quantitative metabolomics, J. Chromatogr., A 1430 (2015) 80–95, https://doi.org/10.1016/j.chroma.2015.12.007.
[23] A.T. Lubben, J. Scott McIndoe, A.S. Weller, Coupling an electrospray ionwization mass spectrometer with a glovebox: a straightforward, powerful, and convenient combination for analysis of air-sensitive organometallics, Organometallics 27 (2008) 3303–3306, https://doi.org/10.1021/om800164e.
[24] K. Benkestock, G. Sundqvist, P.O. Edlund, J. Roeraade, Influence of droplet size, capillary-cone distance and selected instrumental parameters for the analysis of noncovalent protein-ligand complexes by nano-electrospray ionization mass spectrometry, J. Mass Spectrom. (2004), https://doi.org/10.1002/jms.685.
[25] J.S. Page, I. Marginean, E.S. Baker, R.T. Kelly, K. Tang, R.D. Smith, Biases in ion transmission through an electrospray ionization-mass spectrometry capillary inlet, J. Am. Soc. Mass Spectrom. (2009), https://doi.org/10.1016/j.jasms.2009.08.018.
[26] J. Dallüge, R.J.J. Vreuls, J. Beens, U.A.T. Brinkman, Optimization and characterization of comprehensive two-dimensional gas chromatography with time-of-flight mass spectrometric detection (GC × GC - TOF MS), J. Separ. Sci. (2002), https://doi.org/10.1002/1615-9314(20020301)25:4<201::AID-JSSC201>3.0.CO;2-B.
[27] A. Kruve, Influence of mobile phase, source parameters and source type on electrospray ionization efficiency in negative ion mode, J. Mass Spectrom. (2016), https://doi.org/10.1002/jms.3790.
[28] M. Yamashita, J.B. Fenn, Electrospray ion source. Another variation on the free-jet theme, J. Phys. Chem. (1984), https://doi.org/10.1021/j150664a002.
[29] S. Zhou, K.D. Cook, A mechanistic study of electrospray mass spectrometry: charge gradients within electrospray droplets and their influence on ion response, J. Am. Soc. Mass Spectrom. (2001), https://doi.org/10.1016/S1044-0305(00)00213-0.
[30] M.G. Ikonomou, A.T. Blades, P. Kebarle, Electrospray-ion spray: a comparison of mechanisms and performance, Anal. Chem. (1991), https://doi.org/10.1021/ac00018a017.
[31] S.S. Cai, L.C. Short, J.A. Syage, M. Potvin, J.M. Curtis, Liquid chromatography-atmospheric pressure photoionization-mass spectrometry analysis of triacylglycerol lipids-Effects of mobile phases on sensitivity, J. Chromatogr., A (2007), https://doi.org/10.1016/j.chroma.2007.10.008.
[32] G.K. Koyanagi, V. Blagojevic, D.K. Bohme, Applications of extractive electrospray ionization (EESI) in analytical chemistry, Int. J. Mass Spectrom. 379 (2015) 146–150, https://doi.org/10.1016/j.ijms.2015.01.011.
[33] P.A. Steenkamp, N.M. Harding, F.R. van Heerden, B.E. van Wyk, Identification of atractyloside by LC-ESI-MS in alleged herbal poisonings, Forensic Sci. Int. (2006), https://doi.org/10.1016/j.forsciint.2005.11.010.
[34] M. Wilm, M. Mann, Analytical properties of the nanoelectrospray ion source, Anal. Chem. (1996), https://doi.org/10.1021/ac9509519.
[35] A. Cryar, K. Groves, M. Quaglia, Online hydrogen-deuterium exchange traveling wave ion mobility mass spectrometry (HDX-IM-MS): a systematic evaluation, J. Am. Soc. Mass Spectrom. (2017), https://doi.org/10.1007/s13361-017-1633-z.